

A major purpose of the Technical Information Center is to provide the broadest dissemination possible of information contained in DOE's Research and Development Reports to business, industry, the academic community, and federal, state and local governments.

Although a small portion of this report is not reproducible, it is being made available to expedite the availability of information on the research discussed herein.

## NOTICE

**PORTIONS OF THIS REPORT ARE ILLEGIBLE. It  
has been reproduced from the best available  
copy to permit the broadest possible avail-  
ability.**

Los Alamos National Laboratory is operated by the University of California for the United States Department of Energy under contract W-7405-ENG-36.

LA-UR-84-1523-3

TITLE: LITTLE BOY NEUTRON SPECTRUM BELOW 3 MeV

LA-UR--84-1523

DE84 012631

AUTHOR(S): A. E. Evans  
Los Alamos National Laboratory  
Los Alamos, NM 87545

and

E. F. Bennett and T. J. Yule  
Argonne National Laboratory  
Argonne, IL 60439

SUBMITTED TO:  
Annual Meeting of the Health Physics Society  
New Orleans, Louisiana  
June 5, 1984

## DISCLAIMER

This report was prepared as an account of work sponsored by an agency of the United States Government. Neither the United States Government nor any agency thereof, nor any of their employees, makes any warranty, express or implied, or assumes any legal liability or responsibility for the accuracy, completeness, or usefulness of any information, apparatus, product, or process disclosed, or represents that its use would not infringe privately owned rights. Reference herein to any specific commercial product, process, or service by trade name, trademark, manufacturer, or otherwise does not necessarily constitute or imply its endorsement, recommendation, or favoring by the United States Government or any agency thereof. The views and opinions of authors expressed herein do not necessarily state or reflect those of the United States Government or any agency thereof.

By acceptance of this article, the publisher recognizes that the U.S. Government retains a nonexclusive, royalty-free license to publish or reproduce the published form of this contribution, or to allow others to do so, for U.S. Government purposes.

The Los Alamos National Laboratory requests that the publisher identify this article as work performed under the auspices of the U.S. Department of Energy.

118  
DISTRIBUTION OF THIS DOCUMENT IS UNLIMITED



**Los Alamos** Los Alamos National Laboratory  
Los Alamos, New Mexico 87545

## LITTLE BOY NEUTRON SPECTRUM BELOW 3 MeV

A. E. Evans  
Los Alamos National Laboratory  
Los Alamos, NM 87545

E. F. Bennett and T. J. Yule  
Argonne National Laboratory  
Argonne, IL 60439

### ABSTRACT

The leakage neutron spectrum from the Little Boy replica has been measured from 12 keV to 3 MeV using a high-resolution  $^3\text{He}$  ionization chamber, and from 1 keV to 3 MeV using proton-recoil proportional counters. The  $^3\text{He}$ -spectrometer measurements were made at distances of 0.75 and 2.0 m from the active center and at angles of 0°, 45°, and 90° with respect to the axis of the assembly. Proton-recoil measurements were made at 90° to the assembly axis at distances of 0.75 and 2.0 m, with a shielded measurement made at 2.0 m to estimate background due to scattering. The  $^3\text{He}$  spectrometer was calibrated at Los Alamos using monoenergetic  $^7\text{Li}(\text{p},\text{n})^7\text{Be}$  neutrons to generate a family of response functions. The proton-recoil counters were calibrated at Argonne by studying the capture of thermal neutrons by nitrogen in the counters, by observation of the 24-keV neutron resonance in iron, and by relating to the known hydrogen content of the counters. The neutron spectrum from Little Boy was found to be highly structured, with peaks corresponding to minima in the iron total neutron cross section. In particular, influence of the 24-keV iron "window" was evident in both sets of spectra. The measurements provide information for dosimetry calculations and also a valuable intercomparison of neutron spectrometry using the two different detector types. Spectra measured with both detectors are in essential agreement.

### INTRODUCTION

Data relating to the survivors of nuclear weapon explosions are important in the formulation of radiation protection standards. The biological data are, however, of limited use unless the nature and

intensity of radiation from the explosions are well characterized. Although the radiations from the Nagasaki explosion are reasonably well understood, the data from Hiroshima are not. Little Boy, the Hiroshima bomb, was a unique weapon with a radiation output considerably different from that of Fat Man,

which was exploded over Nagasaki. Furthermore, the Little Boy design was never tested in the field. All that is known about its radiation output has been determined from calculations and indirect evidence.

Recently at Los Alamos a replica of Little Boy was built with which one could characterize the radiation produced by the explosion (Malenfant, 1984). This replica, built as a critical assembly, was identical in every way to the original device except that the explosive assembly system was replaced by a precision linear actuator and the mass of  $^{235}\text{U}$  was reduced to a point where the critical system could be safely operated as a low-power steady-state reactor. Measurements of neutron and gamma-ray spectra and dose rates have been made of the radiation output of the replica by many laboratories. This paper discusses  $^3\text{He}$  spectrometer measurements of the neutron spectrum from 0.02 to 3 MeV, and compares these measurements with spectra derived from proton-recoil counter measurements. A preliminary report of the  $^3\text{He}$ -spectrometer results has been given (Evans, 1974). The proton-recoil results will be described in more detail in another paper at this session (Bennett and Yule, 1984).

### $^3\text{He}$ SPECTROMETER MEASUREMENTS

A  $^3\text{He}$  ionization chamber of the type built by Cuttler and Shalev (Cuttler, Shalev, and Dagan, 1969) was used to obtain high-resolution spectra out to 3 MeV. This unit has a sensitive volume 5 cm in diameter by 15 cm long filled with 5 atm of  $^3\text{He}$ , 2 atm of argon, and a few percent of

methane. The stainless steel counter tube is surrounded by a thermal-neutron shield consisting of 2 mm of pressed boron nitride sandwiched between two 0.5-mm-thick layers of cadmium. To suppress acoustic and electrical noise, the chamber plus its attached preamplifier and gas-purifier cell were supported in Styrofoam rings inside a 15-cm-diameter 1-mm-thick aluminum can.

A pulse-height response for 1-MeV neutrons incident upon this detector is shown in Figure 1. The full-energy peak is produced by the  $^3\text{He}(\text{n},\text{p})^3\text{He}$  reaction, which produces ionization in the chamber proportional to the neutron energy plus 765 keV. A continuum of pulses extends downward from the full-energy peak due to events that dissipate part of their energy outside the sensitive volume of the detector (wall and end effects). A continuum of comparable magnitude is produced by proton recoils from the methane in the counter. A larger continuum, caused by elastic scattering from  $^3\text{He}$ , produces pulses up to three-fourths of the neutron energy. This last continuum will override the spectrum being measured when neutrons of energies greater than 1 MeV are present. However, the  $^3\text{He}$ -recoil pulses may be removed from the spectrum by pulse-shape discrimination (Evans and Brandenberger, 1979). The energy dependence of the Little Boy spectrum declined steeply enough with increasing energy that pulse-shape discrimination could usually be dispensed with.

The spectrometer was calibrated using monoenergetic neutrons from the  $^7\text{Li}(\text{p},\text{n})^7\text{Be}$  reaction at the Los Alamos 3.75-MeV Van de Graaff. From a set of response functions

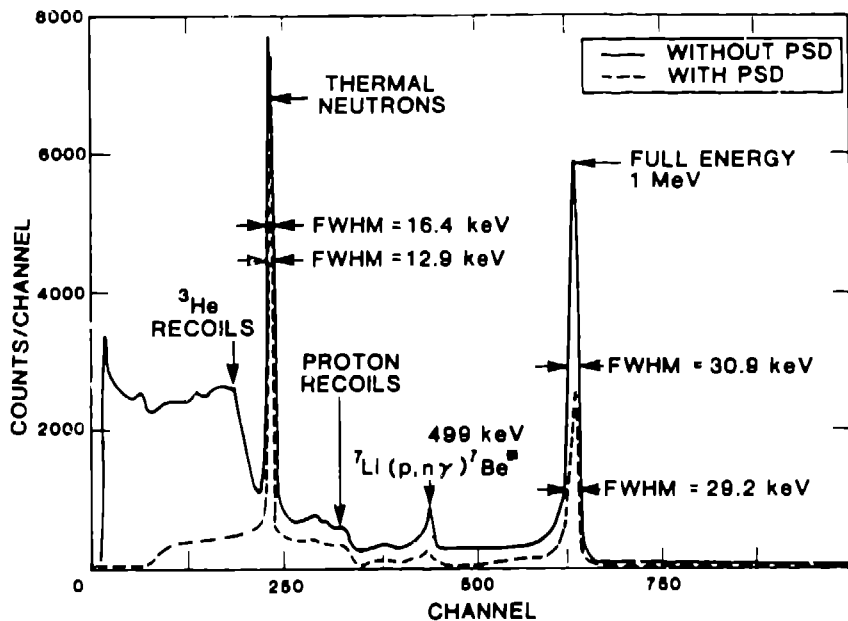


Figure 1. Pulse-height response of the  $^3\text{He}$  spectrometer to 1-MeV neutrons.

for neutrons of energies from 100 to 1200 keV, the full-energy-peak efficiency was obtained as a function of energy, as were coefficients for stripping out wall-effect and proton-recoil contributions to the pulse-height distribution. The peak-efficiency curve was extrapolated below 100 keV using the inverse-velocity dependency of the  $^3\text{He}(n,p)$  cross section. The efficiency above 1 MeV was obtained from a previous calibration.

In Figure 2, we display a pulse-shape-selected pulse-height distribution for a typical spectrum, together with pulses from room-scattered background measured by shielding the direct path from Little Boy to the detector. For this measurement, the Little Boy replica was pointed upwards (i.e., upside down) inside a concrete building with its active core cen-

tered about 2 m above the floor. The nearest wall or ceiling was 4 m distant. The spectrometer tube was located at  $90^\circ$  to the axis of the assembly, at a distance of 0.75 m from the active center. There is little difference except in magnitude between the total and rise-time-selected distributions at energies higher than the epithermal peak. Pulses in the total distribution at energies lower than the epithermal peak are due mostly to  $^3\text{He}$  recoils; pulse-shape selection effectively removes most of these. There was a slight improvement in energy resolution of the pulse-shape-selected distribution compared with the total distribution.

The room-scattered background was found to be mostly epithermal neutrons plus a count-rate-dependent peak at 1528 keV due to simultaneous detection of two epithermal

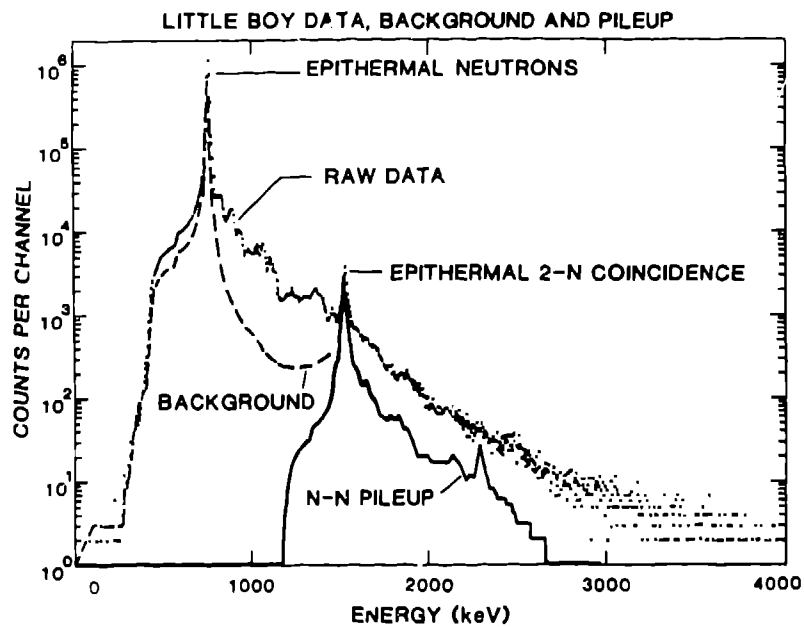


Figure 2. Pulse-shape-selected pulse-height distribution from Little Boy at  $90^\circ$ , 0.75 m, together with the background from room-scattered neutrons and a computed neutron-neutron pileup contribution.

neutrons. The continuum between the epithermal singles and coincidence peaks is attributable almost entirely to wall effect from coincident epithermal events and to un-suppressed pileup (a pileup inspection circuit removed approximately 90% of initial pileup). For measurements at other positions, the net area of the coincidence peak was used as a measure of scattered background and the indicated background was normalized to remove this peak from the raw pulse-height distribution. This made very little difference in the shape of the spectrum except in the vicinities of these two peaks.

In addition to the epithermal-neutron coincidence peak, there is a pileup distribution of energetic neutrons coincident with the epi-

thermal background. This distribution is an image of the singles distribution, reduced in intensity, shifted 764 keV upwards, and slightly broadened in energy resolution. The contribution  $P_k$  of this pileup in channel  $k$  can be represented by

$$P_k = \tau \sum_{j=1}^k n_j n_{k-j} ,$$

where  $n_j$  and  $n_{k-j}$  are the counting rates in channels  $j$  and  $k-j$ , respectively, and  $\tau$  is the coincidence resolving time of the system. In practice, one may take the  $n_j$ 's to be the total counts in each channel and adjust  $\tau$  to just remove

the epithermal coincidence peak from the spectrum: i.e.,

$$\tau = \frac{N_{th}(2)}{[N_{th}(1)]^2},$$

where  $N_{th}(2)$  is the net area of the epithermal coincidence peak and  $N_{th}(1)$  is the area of the epithermal singles peak. The contribution of this neutron-neutron pileup is shown in Figure 2.

After subtraction of background, the data were corrected for wall-effect and proton-recoil distributions. The resultant pulse-height distribution was divided by the measured energy-dependent pulse-shape-selected full-energy-peak efficiency and shifted in energy by the Q-value of the  ${}^3\text{He}(n,p){}^3\text{H}$  reaction to produce the finished spectrum. A FLEXTRAN™ program has been written to permit execution of these calculations within the TN-4000\* multichannel-analyzer system.

In Figure 3, the spectrum from 0 to 1 MeV is shown. Also shown in the figure is the ENDF/B-V total neutron cross-section for iron. All of the indicated peaks in the spectrum correspond to prominent minima in the iron cross-section. In particular, approximately 15% of the neutrons above the epithermal peak are to be found in the 24-keV iron window, which is often used to produce a nearly monoenergetic 24-keV neutron beam at reactor facilities. The results are consistent with the length of iron that the neutrons penetrate.

\*FLEXTRAN is a programming language copywritten by Tracor-Northern, Inc., of Middleton, Wisconsin.

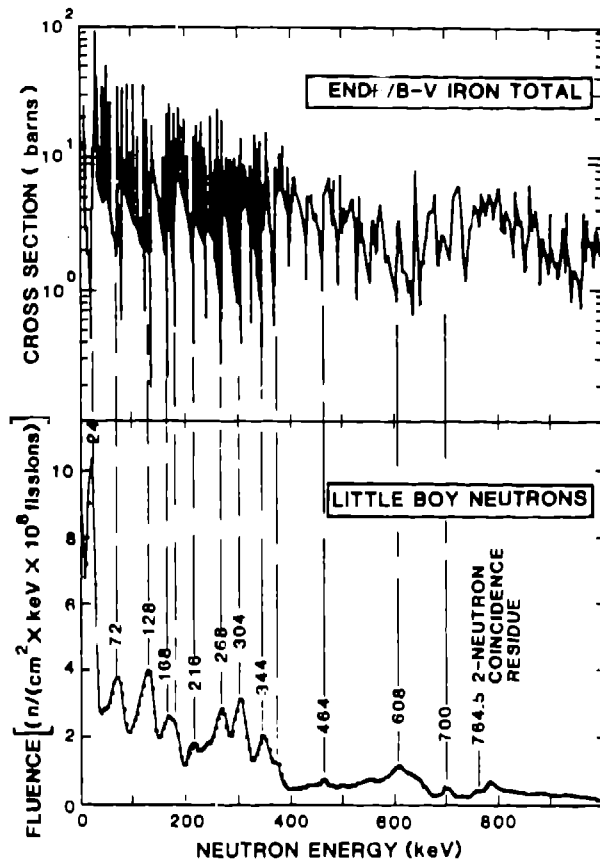


Figure 3. Spectrum 0- to 1-MeV compared with the ENDF/B-B total cross-section for iron.

Spectra were also measured at the outdoor installation of the replica at distances of 0.75 and 2.0 m and at angles of 0°, 45°, and 90° with respect to the assembly axis. These spectra are shown in Figures 4 and 5. There is a slight hardening of the 90° spectra compared to spectra on axis and, of course, a large difference in total magnitude due to the increased path length through iron in the forward direction as compared to the side. The only background subtracted from these spectra was a reconstruction of the two-neutron coincidence peak and its associated wall effect.

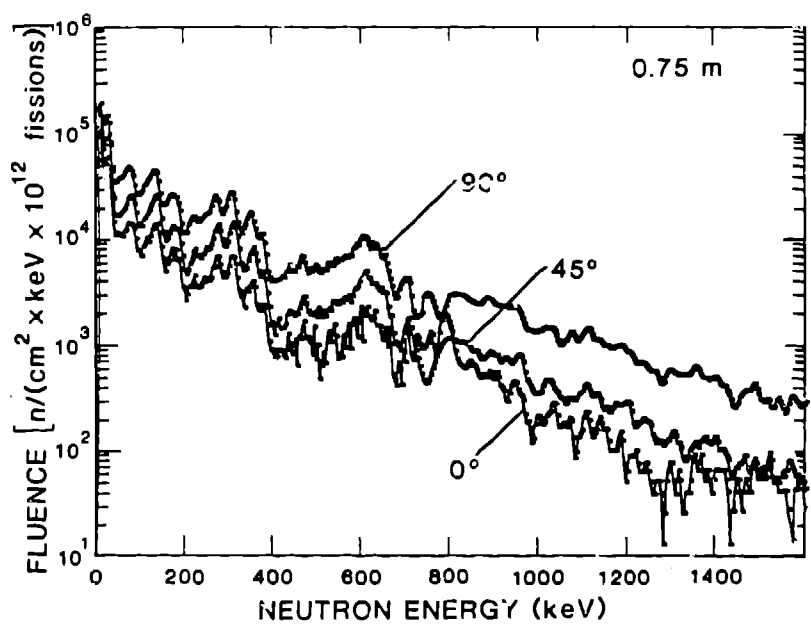


Figure 4. Neutron spectra at 0.75 m.

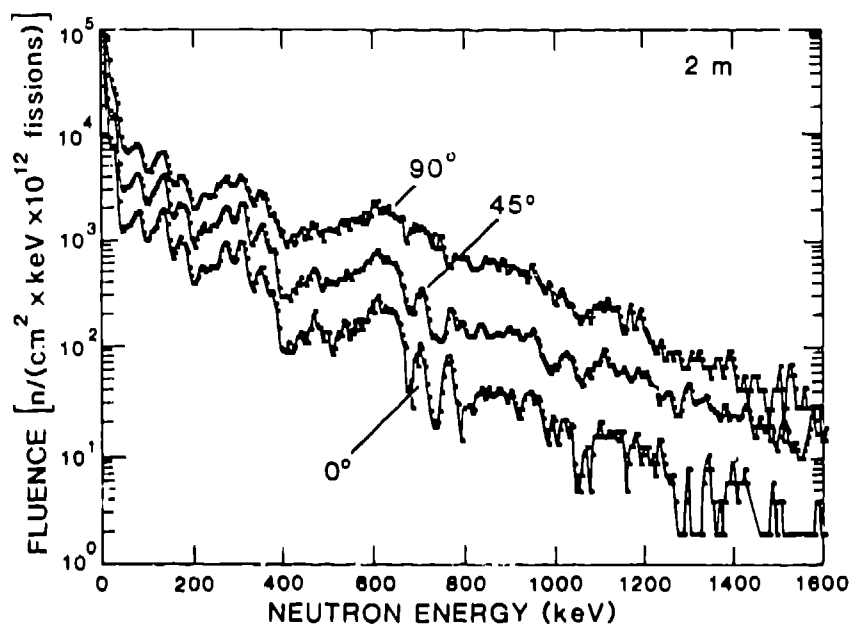


Figure 5. Neutron spectra at 2.0 m.

TABLE 1. Neutron Dosages from Little Boy

Energy Range (keV)	Dose in Energy Interval (rem/10 <sup>20</sup> fissions) for Source-to-Detector Distance at Given Angle					
	0.75 m, 90°	0.75 m, 45°	0.75 m, 0°	2.0 m, 90°	2.0 m, 45°	2.0 m, 0°
12 - 40	4.92 x 10 <sup>5</sup>	3.95 x 10 <sup>5</sup>	2.40 x 10 <sup>5</sup>	1.26 x 10 <sup>5</sup>	5.70 x 10 <sup>4</sup>	2.88 x 10 <sup>4</sup>
40 - 200	3.45 x 10 <sup>6</sup>	1.83 x 10 <sup>6</sup>	1.03 x 10 <sup>6</sup>	5.97 x 10 <sup>5</sup>	3.15 x 10 <sup>5</sup>	1.44 x 10 <sup>5</sup>
200 - 400	5.12 x 10 <sup>6</sup>	2.46 x 10 <sup>6</sup>	1.24 x 10 <sup>6</sup>	9.50 x 10 <sup>5</sup>	4.48 x 10 <sup>5</sup>	1.88 x 10 <sup>5</sup>
400 - 676	4.69 x 10 <sup>6</sup>	1.94 x 10 <sup>6</sup>	9.12 x 10 <sup>5</sup>	1.18 x 10 <sup>6</sup>	3.86 x 10 <sup>5</sup>	1.27 x 10 <sup>5</sup>
676 - 1000	2.76 x 10 <sup>6</sup>	9.32 x 10 <sup>5</sup>	7.92 x 10 <sup>5</sup>	8.35 x 10 <sup>5</sup>	1.79 x 10 <sup>5</sup>	4.52 x 10 <sup>4</sup>
1000 - 1500	1.40 x 10 <sup>6</sup>	3.73 x 10 <sup>5</sup>	1.84 x 10 <sup>5</sup>	2.57 x 10 <sup>5</sup>	8.35 x 10 <sup>4</sup>	1.59 x 10 <sup>4</sup>
1500 - 2000	3.68 x 10 <sup>5</sup>	6.78 x 10 <sup>4</sup>	1.85 x 10 <sup>4</sup>	4.43 x 10 <sup>4</sup>	2.46 x 10 <sup>4</sup>	2.52 x 10 <sup>3</sup>
0 - 2000	1.82 x 10 <sup>7</sup>	7.85 x 10 <sup>6</sup>	4.47 x 10 <sup>6</sup>	3.99 x 10 <sup>6</sup>	1.50 x 10 <sup>6</sup>	5.71 x 10 <sup>5</sup>

produced by taking the difference of two spectra of the same source measured at different counting rates. There are some irregularities in the spectra in the vicinity of 765 keV due to count-rate-dependent gain and resolution shifts of the synthesized background peak.

These spectra have been converted into neutron dose spectra, using the ANSI 6.1.1 neutron flux-to-dose-rate factors (American Nuclear Society, 1971). The results of conversion of the data shown in Figures 4 and 5, integrated over energy regions selected to place energy boundaries at spectral minima, are shown in Table 1. This tabulation is intended to facilitate comparison of the neutron spectra with integral dosimetry measurements that have been made at the same positions. The results show that the median dose occurs at between 300 and 500 keV, whereas the median neutron flux energy varies from 30 to 150 keV.

#### COMPARISON WITH PROTON RECOIL MEASUREMENTS

Linear and semi-logarithmic comparisons of the <sup>3</sup>He data with data from proton-recoil measurements are displayed in Figures 6 and 7. The proton-recoil measurements were made with two 2.5-cm-diam by 7.6-cm-long proportional counters, one filled with methane and the other with hydrogen. Pulse-shape analysis and established analytical techniques (Bennett and Yule, 1971) were used to reduce the pulse-height distributions to neutron spectra. The efficiencies of these counters as a function of energy have been derived principally from calculations. Experimental checks of response functions were made by observing the response function of the 615-keV deposition of ions from capture of thermal neutrons by nitrogen in the counters. The same reaction provides for energy calibration in the field.

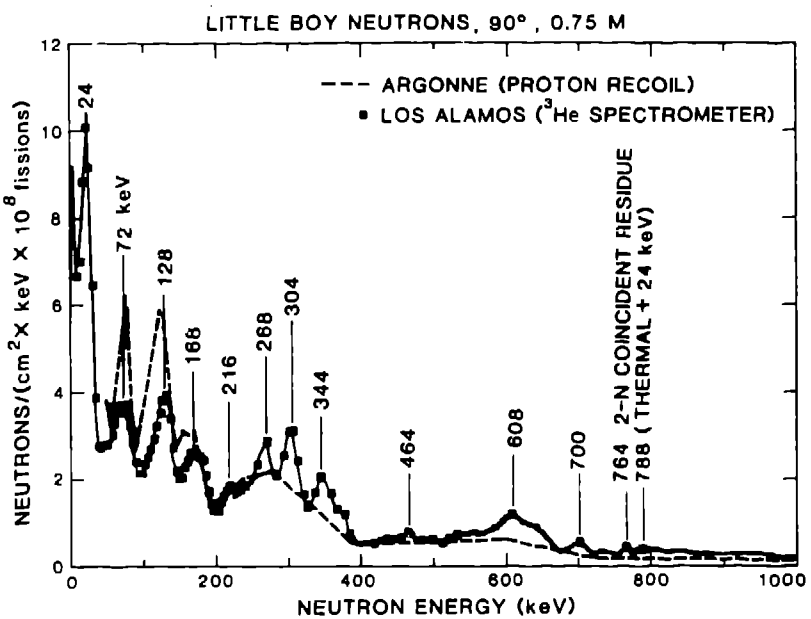


Figure 6. Comparison of measurements of the 0- to 1-MeV neutron from Little Boy with  $^3\text{He}$  and proton-recoil spectrometers.

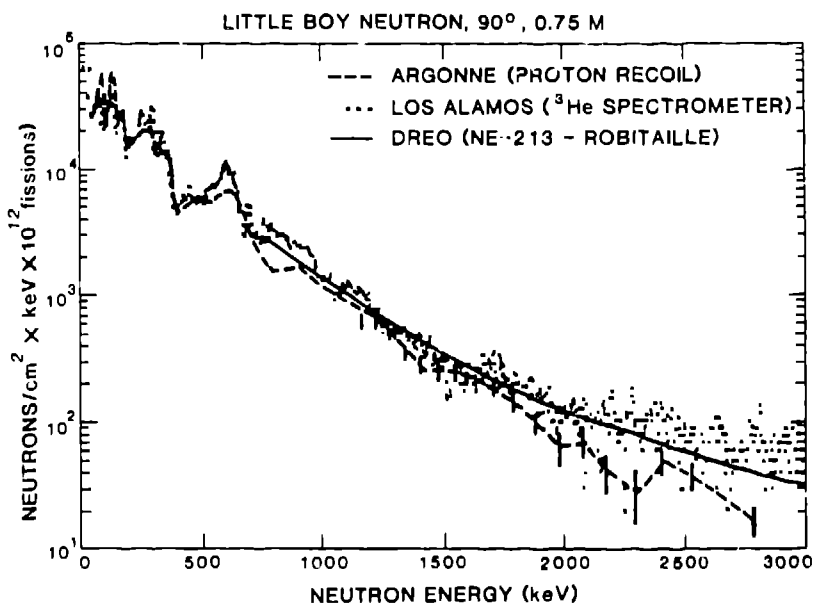


Figure 7. Logarithmic display of 0- to 3-MeV neutron spectra measured with  $^3\text{He}$  and proton-recoil spectrometers.

TABLE 2. Comparison of the  $^3\text{He}$  and Proton-Recoil-Derived Little Boy Neutron Spectra at 90°, 0.75 m (Fluence Units Are Neutrons/cm<sup>2</sup>/10<sup>12</sup> Fissions)

Interval (keV)	Fluence in Interval		$^3\text{He}$ Proton Recoil
	$^3\text{He}$ Spectrometer	Proton Recoil Spectrometer	
8-40	$2.19 \times 10^6$	$2.28 \times 10^6$	0.96
40-96	$1.91 \times 10^6$	$1.69 \times 10^6$	0.88
92-152	$1.72 \times 10^6$	$2.33 \times 10^6$	0.74
148-200	$1.11 \times 10^6$	$1.25 \times 10^6$	0.89
204-416	$3.68 \times 10^6$	$3.20 \times 10^6$	1.15
420-580	$7.07 \times 10^6$	$1.10 \times 10^6$	0.97
580-680	$3.35 \times 10^5$	$5.96 \times 10^5$	1.20
684-1000	$4.09 \times 10^5$	$3.60 \times 10^5$	1.14
804-1008	$4.96 \times 10^5$	$3.78 \times 10^5$	1.31
1012-1564	$3.68 \times 10^5$	$3.31 \times 10^5$	1.11
1568-2096	$9.66 \times 10^4$	$8.34 \times 10^4$	1.16
2100-2952	$6.75 \times 10^4$	$2.79 \times 10^4$	2.45

In Table 2, the  $^3\text{He}$  and proton-recoil measurements of the Little Boy spectrum are compared, integrated over selected energy intervals. There has been no renormalization of either the  $^3\text{He}$  or the proton-recoil spectra. Agreement is generally good up to 2 MeV. Below 150 keV, Figure 6 appears to show a divergence of the two spectra with the proton-recoil counter showing a higher fluence at lower energies. However, the differential curves are deceptive, because the energy resolution of the proton-recoil counter is better than that of the  $^3\text{He}$  spectrometer for energies less than 150 keV. The  $^3\text{He}$  spectrometer resolution (FWHM) in this region is about 15 keV, whereas the proton-recoil counter resolution, which varies from 10 keV at

100 keV to 400 eV at 1 keV, is 3 keV for 24-keV neutrons. The proton-recoil-counter spectrum peaks at  $3.5 \times 10^5$  neutrons/(cm<sup>2</sup> · keV · 10<sup>12</sup> fissions) (not shown in Figures 6 and 7), whereas the corresponding value for the  $^3\text{He}$  counter is  $1.03 \times 10^5$ . However, as one can see from Table 2, integration over the 24-keV peaks for both detectors gives equivalent fluences. Likewise, the areas of the 72-, 128-, and 168-keV peaks agree within from 12 to 25%.

There is evidence of a small bias at energies higher than 764 keV, the  $^3\text{He}$ -spectrometer results being on the average somewhat higher. This is particularly evident between 800 and 950 keV, and may indicate that some coincidence pileup

events, possibly between  $^3\text{He}$  recoils are leaking through the pulse-shape selection system. It is possible that two overlapping  $^3\text{He}$  recoil pulses or a  $^3\text{He}$ -recoil plus a proton capture could have a risetime characteristic of a pure  $^3\text{He}(n,p)$  pulse and thus be accepted for the shape-selected distribution. However, the  $^3\text{He}$  data above 800 keV are more consistent with those of Robitaille and Hoffarth (1983).

### CONCLUSION

The intercomparison of this work with the liquid scintillator measurements of Robitaille and Hoffarth from 600 keV to 10 MeV (Robitaille and Hoffarth, 1983) and with measurements using Bonner Spheres and Track etch techniques should provide a well-characterized source spectrum for the calculation of Little Boy dose measurements. It should also be a valuable intercomparison of different techniques and different laboratories of neutron spectrometry.

### ACKNOWLEDGMENTS

We wish to thank the following people who participated in the operation of the Little Boy assembly and in the execution of this experiment: M. B. Diaz, H. M. Forehand, G. E. Hansen, R. E. Malenfant, R. A. Pederson, B. Pena, E. A. Plassmann, and T. F. Wimett.

### REFERENCES

American Nuclear Society. 1977. Neutron and Gamma-Ray Flux-to-Dose-Rate Factors. American National

Standards Institute ANSI/ANS-6.1.1-1977 (N666).

Bennett, E. F., and T. J. Yule. 1971. Techniques and Analyses of Fast-Reactor Neutron Spectroscopy with Proton-Recoil Counters. Argonne National Laboratory report ANL-7763.

Bennett, E. F., and T. J. Yule. 1984. "Neutron Spectra Measurements of the Replica of the Little Boy Using Proton Recoil Counters." Annual Meeting of the Health Physics Society, New Orleans, June 5, 1984.

Cuttler, J. M., S. Shalev, and Y. Dagan. 1969. "A High-Resolution Fast-Neutron Spectrometer." Trans. Am. Nucl. Soc. 12(1):63.

Evans, A. E., and J. D. Brandenberger. 1979. "High Resolution Fast Neutron Spectrometry Without Time-of-Flight." IEEE Trans. Nucl. Sci. NS-26(1): 1484-1486.

Evans, A. E. 1984. "Little Boy Neutron Spectrum Below 1 MeV." Proceedings of the Seventeenth Midyear Topical Symposium of the Health Physics Society, 8.29-8.36.

Malenfant, R. E. 1984. "Little Boy Replication: Justification and Construction." Proceedings of the Seventeenth Midyear Topical Symposium of the Health Physics Society, 8.1-8.4, and the Annual Meeting of the Health Physics Society, New Orleans, June 5, 1984.

Robitaille, H. A. and B. E. Hoffarth. 1983. Neutron Leakage from "Comet"--A Duplicate Little Boy Device. DREO Report R-878, Defense Research Establishment Ottawa, Ottawa, Canada.